Thermal Science and Engineering Progress 54 (2024) 102793

Contents lists available at ScienceDirect

Thermal Science and Engineering Progress

journal homepage: www.sciencedirect.com/journal/thermal-science-and-engineering-progress

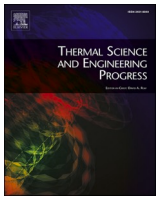

Energy-exergy-economic-environmental (4E) analysis and multi-objective optimization of a cascade refrigeration system

Parth Prajapati [a], Vivek Patel [a], Bansi D. Raja [b], Hussam Jouhara [c,d]

[a] Department of Mechanical Engineering, Pandit Deendayal Energy University, Gandhinagar 382421, Gujarat, India
[b] Department of Mechanical Engineering, Indus University, Ahmedabad, Gujarat, India
[c] Heat Pipe and Thermal Management Research Group, College of Engineering, Design and Physical Sciences, Brunel University London, UB8 3PH, UK
[d] Vytautas Magnus University, Studentu Str. 11, LT-53362 Akademija, Kaunas Distr., Lithuania

ARTICLE INFO

Keywords:
Cascade refrigeration cycle
Multi-objective optimization
TOPSIS
4E analysis

ABSTRACT

The present work focusses on 4E analysis of a 50 kW cooling capacity cascade refrigeration cycle covering the aspects of energy, exergy, economic and environment analysis. The numerical investigation and the multi-objective optimization is carried out for the system using the refrigerant pair R170-R600a and R41-R600a. The refrigerant pair is selected based on the environmental implications in terms of GWP and ODP. Multi-objective optimization of the objective functions is carried out using a heat transfer search optimization algorithm to evaluate the optimal performance of the system. The effect of evaporator temperature, condenser temperature, LTC condenser temperature and LTC condenser temperature difference on the exergy efficiency and total cost of the system is studied. A set of multiple optimal solutions is presented using the Pareto optimal curve and TOPSIS criteria is employed to select the optimal operating condition. Compared to the refrigerant pair R170-R600a, the system with R41-R600a operates at better exergy efficiency and lower total cost. At the TOPSIS selected optimal condition, exergy efficiency and the total cost of the CRS is 63.5 % and 65,228 $/year for the refrigerant pair R41-R600a and 62.6 % and 67,690 $/year for R170-R600a, respectively. The distribution of variables shows that the effect of the evaporation temperature, condensation temperature and the LTC condenser temperature is profound in obtaining the optimal solution.

1. Introduction

The growing need for refrigeration due to the necessity of daily human comfort, machine comfort, and food preservation for a longer duration has motivated researchers to develop energy and cost-efficient refrigeration systems [1]. Researchers are also looking forward to using environmentally friendly and economical refrigerants considering global warming and carbon emissions. Domestic appliances like refrigerators, heat pumps, and air-conditioners primarily operate on a vapour compression refrigeration cycle (VCR) with lower temperature lift. In many engineering applications like chemical, pharmaceutical, poultry, and frozen food industries, the temperature requirement can be as low as −35 ℃ to −70 ℃ [2,3,4]. In such applications, the temperature lift is substantially high due to extremely low evaporator temperature or due to high condensing temperature (hot climate).

During such high cooling loads, the simple vapour compression refrigeration system working as a single stage is unfavourable due to increased compressor work input and lower COP of the system. To overcome the problem of high-temperature lift, a cascade refrigeration system (CRS) can be employed that uses two VCR systems in series, and eventually, lower evaporator temperatures can be attained [5]. It is similar to a multiple-stage system with the only change that refrigerants can be different in both stages. The system comprises two circuits, namely a high-temperature circuit (HTC) and a low-temperature circuit (LTC), using different refrigerant pairs. Concerning the development of energy-efficient, cost-effective, and environmentally friendly systems, considerable attention has been devoted to optimizing CRS along with the optimum selection of working fluids. The use of refrigerants with zero ODP and relatively low GWP is given prime importance in industries to reduce greenhouse emissions and avoid harm to the ozone layer [6,7,8]. Numerous studies have been carried out to understand the performance of CRS using energetic and exergetic approaches. Along with the efforts in improving the performance of CRS, studies have been carried out with a focus on a selection of refrigerant pairs to have minimal impact on the environment.

Singha et al. [9] performed a study to enhance the performance of CRS and minimize the environmental impact of CRS by using parallel

E-mail addresses: vivekp@sot.pdpu.ac.in (V. Patel), Hussam.Jouhara@brunel.ac.uk (H. Jouhara).

https://doi.org/10.1016/j.tsep.2024.102793
Received 26 April 2024; Received in revised form 23 July 2024; Accepted 10 August 2024
Available online 12 August 2024

Nomenclature

Abbreviations

A	Area (m^2)
U	Overall heat transfer coefficient (W/m^2K)
Q	heat transfer, (kW)
h	specific enthalpy, (kJ/kg)
s	specific entropy, (kJ/kg K)
W_{comp}	compressor work, (kJ/kg)
ED	Exergy destruction
η_{ex}	exergy efficiency
i	population size
j	design variable
g	number of generations
$S_{y,x}$	updated solution (objective function value)
$S_{z,z}$	randomly selected solution from the population
R	probability of executing a phase
r	random number between [0,1]
CRS	Cascade refrigeration system
VCR	Vapour compression refrigeration
LTC	Low temperature circuit
HTC	High temperature circuit
COP	Coefficient of performance
CDF	conduction factor
COF	convection factor
RDF	radiation factor
HTS	Heat transfer search
ODP	Ozone Depletion Potential
GWP	Global Warming Potential

compression in LTC, a gravity fed evaporator and an ejector in HTC. The study also aimed to avoid the use of synthetic refrigerants and use R744 and R290 in LTC and HTC, respectively. Massuchetto et al. [10] evaluated the thermodynamic performance of a CRS with different refrigerant mixtures R744/R1270, R744/R717, and R744/RE170. The results showed that a higher COP could be achieved using mixed refrigerants compared to pure refrigerant fluids. The system yields the highest COP of 2.34 when operated with the refrigerant pair R744/RE170 with 20 wt % R744 in HTC and 10 wt% R744 in LTC. Ustaoglu et al. [11] performed a parametric study of cascade vapour compression refrigeration system using Taguchi and ANOVA methods. The optimum operating conditions were identified for the maximum COP and exergy efficiency of the cascade system. The study proved that the most influential parameters affecting the COP and the exergy efficiency are the evaporator temperature, LTC condenser temperature, condenser temperature of the overall cycle, and the isentropic efficiency of the compressor. In an experimental investigation carried out by Zhang et al. [12], it was observed that the effect of evaporation and condensation temperature is significant on the COP. With the increasing evaporation temperature at constant condensation temperature, COP increases and when the condensation temperature increases at constant evaporation temperature, COP decreases.

Mofrad et al. [13] carried out 4E analyses and multi objective analysis on CRS system with the waste heat recovery system. The high magnitude of heat rejection from the gas cooler is utilized to operate a Rankine cycle for power generation. Further, a genetic algorithm is used to optimise the exergy efficiency, total product cost, COP and product environmental impact. Mahdi et al. [14] presented an energy-exergy-economic-environmental model for a CRS operating with six pairs of refrigerants. The careful selection of refrigerant pairs was done with minimum GWP to minimize the environmental impact of leaking. With the suitable refrigerant pair, CRS could operate at maximum exergy efficiency and COP of 35.3 % and 2.09, respectively. Yilmaz et al. [15] carried out a thermodynamic investigation for energy and exergy efficiency of a cascade cooling system (CCS) using CO_2 and HFE7000 refrigerants. The results were comprehensively at par with the system using refrigerant R134a and it was concluded that HFE7000 can be a good alternative for CCS. In another study by Yilmaz et al. [16] performed a thermodynamic analysis of cascade systems for cooling and heating applications with multiple environment-friendly refrigerants. Among many of the combinations, refrigerant HFE7000 was effective for heating and cooling applications because of the GWP, ODP values and efficiencies. Faruque et al. [17] recommended heptane and toluene as suitable refrigerants for triple cascade vapour refrigeration systems for ultra-low temperature applications. Evaporation temperature, LTC condensation temperature and HTC condensation temperature were considered as the design and operating parameters. For the evaporator temperature of −100 °C, the highest COP and exergy efficiency were calculated to be 0.5931 and 54.446 %, respectively. Singh et al. [18] used natural refrigerants in a cascade refrigeration system incorporated with a flash tank and a flash intercooler with an indirect subcooler. An analysis is carried out to compare the performance of the refrigerants on the basis of exergy efficiency, exergy destruction and system cost rate. From the thermodynamic and economic perspectives, the refrigerant pair R717-R290 showed better results compared to other pairs with the maximum COP and exergy efficiency of 1.9 and 39.1 %. Gill et al. [19] performed an exergy analysis of a vapour compression refrigeration system with the objective of replacing the conventional refrigerant R134a with R450A. The experiments showed that the total irreversibility and exergy efficiency of the system are lower and higher by 15.2–27.3 % and 10.1–130.9 % when operated with R450A as compared to R134a, respectively.

Most of the engineering problems come with multiple constraints and challenges that should be addressed simultaneously. Often the objective functions of the system are conflicting in nature. For such scenarios multi-objective optimization can be employed to optimize the system behaviour for a given number of variables and the effect of individual variables can be studied simultaneously. Roy et al. [20] used a genetic algorithm to maximize the exergy efficiency and minimize the total plant cost rate of CRS working with four different refrigerant pairs. Improved results were obtained with the refrigerant pair R41-R161 and R170-R161. Sun et al. [21] performed a detailed analysis of a cascade refrigeration system with two-stage compression for applications in industries. The objective was to replace the three-stage cascade refrigeration system with a two-stage compression refrigeration system using the refrigerant pair R1150/R717. Gill et al. [22] used an artificial neural network approach to perform an exergy analysis of a vapour compression refrigeration system with the refrigerant blend of R134a/LPG. The neural network models were developed to predict the total irreversibility and the results were compared with the experimental results.

Even though a sufficient amount of experimental work and simulation study has been carried out to improve the performance of CRS, there exists a substantial research gap looking after the strict environmental policies. The selection of a pair of working fluids is an area yet to be explored and the wise selection of the fluids can lead to substantial reduction in greenhouse gas emissions. The extensive research has been carried out with different fluids and the hydrocarbon-based refrigerants with low GWP are still gaining attention. It is of interest to test the system performance using such refrigerants causing minimum impact to the environment.

The major contributions of the current study are: 1) to investigate the effect of refrigerant pair R170-R600a and R41-R600a on the system performance of CRS 2) an in-depth analysis of the CRS from four different perspectives like energy, exergy, economic and environmental

3) to obtain multiple solutions and optimal points satisfying the boundary conditions of individual design variables 4) to understand the effect of design variables on the performance of CRS and 5) to understand the population distribution of design variables to obtain the optimal solutions. The novelty of the work lies in optimizing the system performance using the refrigerant pair which is less harmful to the environment without compromising on the cooling capacity. The analysis is multi-dimensional and covers all the aspects thermodynamically, economically and environmentally.

The current work is organized in the following manner. The detailed description and mathematical modelling are presented in Section 2. Section 3 describes the multi-objective optimization method used in the present work. Section 4 discusses the results of the optimization and the effect of design variables on the overall performance. Section 5 highlights the major findings and conclusions of the proposed work.

2. System description and thermo-economic analysis

In the current section, the working of a conventional cascade refrigeration system is explained in brief. Further, the thermo-economic analysis carried out to understand the effect of design variables on the system performance is discussed. The equations used for the energy and exergy analysis are presented. The schematic diagram of a CRS system is represented using Fig. 1.

The cascade refrigeration system comprises two individual vapour compression refrigeration cycles connected in series. The series connection is ensured by employing a cascade heat exchanger. The system can be subsequently divided into the low-temperature circuit (LTC) and the high-temperature circuit (HTC). The cascade heat exchanger mounted in the system behaves as a condenser in the LTC and an evaporator in the HTC. Thermodynamically, the heat is transferred from the LTC refrigerant to the HTC refrigerant in a cascade condenser. In the current study, refrigerants R41 and R170 are used in the LTC, whereas refrigerant R600a is used in the HTC. The thermophysical properties of the refrigerants used in the cascade refrigeration system are tabulated in Table 1.

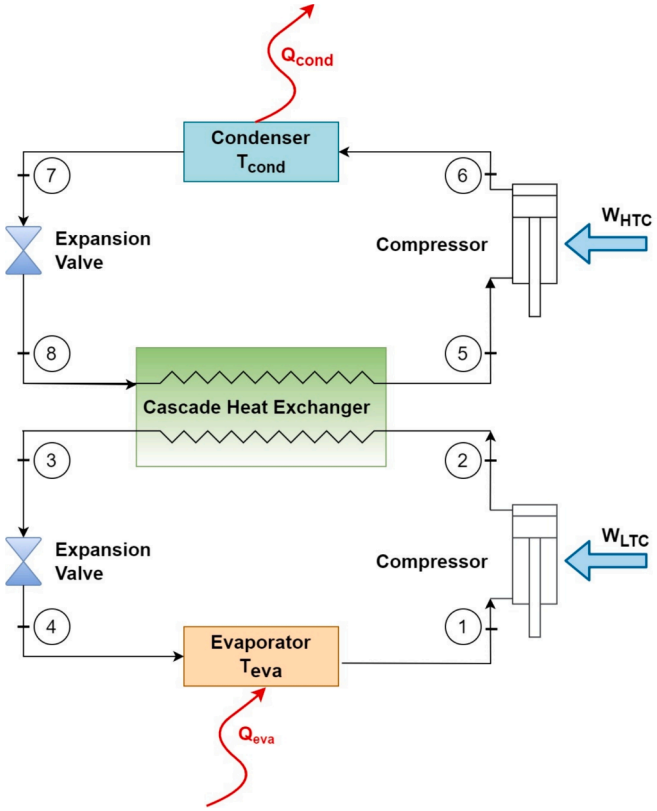

Fig. 1. Schematic diagram of a cascade refrigeration system.

In the LTC, the refrigerant in the evaporator absorbs the heat energy Q_{eva}, from the surroundings providing the required cooling effect at the temperature T_{eva}. Upon absorbing the heat energy, the refrigerant gets evaporated and the vapour refrigerant is supplied to the compressor wherein the pressure of the refrigerant is increased from P_1 to P_2. The compression process is considered to be irreversible and to compress the vapor refrigerant, W_{LTC} amount of work is consumed by the compressor. From the exit of the compressor, the vapour refrigerant goes to the cascade heat exchanger wherein, the heat transfer, Q_{cas} takes place between the LTC refrigerant and HTC refrigerant. For the LTC, the cascade heat exchanger acts as a condenser and for the HTC, it acts as an evaporator. The LTC refrigerant loses the heat energy to the HTC refrigerant at temperature T_{cas} and condenses to liquid form. Simultaneously, the HTC refrigerant absorbs the energy in the cascade heat exchanger and gets converted to vapour. The condensed LTC refrigerant is supplied to the expansion valve to undergo the throttling process resulting in the sudden drop in the pressure and temperature of the LTC refrigerant. The low-temperature liquid refrigerant is then supplied to the evaporator to absorb the heat energy in the LTC and the cycle repeats.

The vaporized HTC refrigerant from the cascade heat exchanger is supplied to the HTC compressor and W_{HTC} amount of work is consumed to increase the pressure from P_5 to P_6. The high-pressure and high-temperature superheated refrigerant enters the condenser wherein it rejects heat energy Q_{cond} to the heat sink at the temperature T_{cond} and gets condensed to the liquid state. The high-pressure, high-temperature liquid HTC refrigerant passes through the expansion valve and the pressure of the refrigerant drops to the evaporator pressure in HTC. The processes carried out in the cascade refrigeration system are presented using a *P-h* diagram as shown in Fig. 2.

During the energy and exergy analysis, the following assumptions are taken into consideration.

- The system components of the cascade refrigeration system run at a steady state condition.
- During the calculations, the change in the value of kinetic and potential energies of the refrigerant is considered to be negligible.
- During the flow of the refrigerant, the pressure drop within the pipelines is neglected.
- The system components do not exchange heat with the surroundings.

2.1. Energy analysis

To understand the system's performance, thermodynamic analysis of individual components of the system is carried out. Energy balance equations are applied at the steady state conditions as mentioned in Table 2.

The compressor is employed in the high-temperature circuit and low-temperature circuit and hence the total compressor power is calculated as,

Table 1
Thermo-physical properties of refrigerants used in the CRS.

	Refrigerants			
	R41	**R170**	**R404a**	**R600a**
Molecular mass, g/mol	34	30	97.6	58.1
Critical temperature, K	317.1	305.3	345.1	407
Boiling point, K	194.7	184.4	226.4	261.3
ASHRAE safety code	A2	A3	A1	A3
ODP	0	0	0	0
GWP	107	20	3800	3

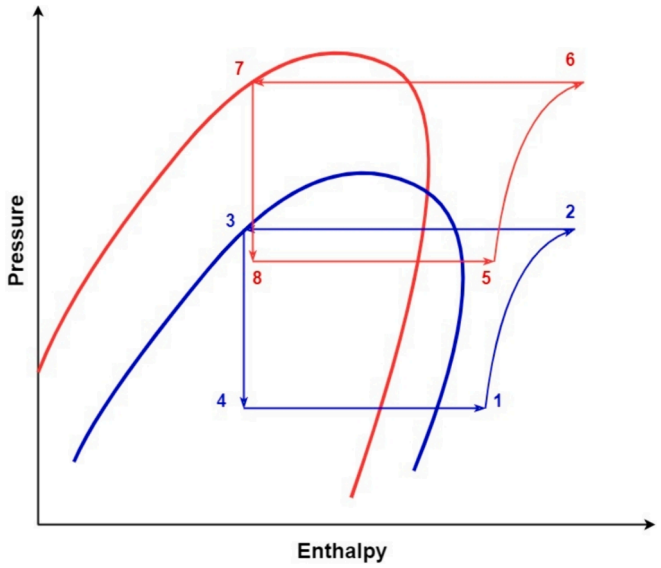

Fig. 2. P-h diagram of the cascade refrigeration system.

Table 2
Energy and exergy analysis of individual components of cascade refrigeration system [25].

Component	Energy analysis	Exergy analysis
Evaporator	$Q_{eva} = \dot{m}_{LTC}(h_1 - h_4)$	$ED_{eva} = Ex_4 - Ex_1 + Q_{eva}\left(1 - \frac{T_o}{T_{eva}}\right)$
Condenser	$Q_{cond} = \dot{m}_{HTC}(h_6 - h_7)$	$ED_{cond} = Ex_6 - Ex_7 + Q_{cond}\left(1 - \frac{T_o}{T_{cond}}\right)$
Cascade condenser	$Q_{cas} = \dot{m}_{LTC}(h_2 - h_3) = \dot{m}_{HTC}(h_5 - h_8)$	$ED_{cas} = Ex_2 + Ex_8 - Ex_3 - Ex_5$
LTC Compressor	$W_{LTC} = \frac{\dot{m}_{LTC}(h_2 - h_1)}{\eta_S x \eta_m x \eta_{elec}}$	$ED_{comp,LTC} = Ex_1 - Ex_2 + W_{LTC}$
HTC Compressor	$W_{HTC} = \frac{\dot{m}_{HTC}(h_6 - h_5)}{\eta_S x \eta_m x \eta_{elec}}$	$ED_{comp,HTC} = Ex_5 - Ex_6 + W_{HTC}$
LTC Throttle valve	$h_3 = h_4$	$ED_{exp,LTC} = Ex_3 - Ex_4$
HTC Throttle valve	$h_7 = h_8$	$ED_{exp,HTC} = Ex_7 - Ex_8$

$$W_{comp} = W_{HTC} + W_{LTC} \tag{1}$$

The heat transfer area of heat exchangers i.e., evaporator, condenser and cascade condenser is calculated as,

$$A = \frac{Q}{UX LMTD} \tag{2}$$

where Q is the magnitude of heat transfer in the heat exchanger, U is the overall heat transfer coefficient; and LMTD is the logarithmic mean temperature difference between two fluid streams.

For a cascade refrigeration system, the coefficient of performance (COP) is an appropriate measure to determine the system's performance. COP of the system is defined as the ratio of the amount of heat transfer in the evaporator to the total work input in the compressor.

$$COP = \frac{Q_{eva}}{W_{total}} \tag{3}$$

2.2. Exergy analysis

The maximum deliverable work output, when the system undergoes a transition from the initial specified state to the dead state is referred to as the exergy of the system [23]. The dead state is referred to as a state when the system is in thermodynamic equilibrium with the environment. Exergy of the system at a specific state point can be calculated using Eq. (4) [24],

$$E_x = \dot{m}\left[(h - h_o) - T_o(s - s_o)\right] \tag{4}$$

where, $\dot{m}$ represents the mass flow rate of the working fluid, h and s represent specific enthalpy and specific entropy at a state point; and h_o, s_o and T_o represent specific enthalpy, specific entropy and temperature of the dead state.

Total exergy destruction of the system is the summation of individual component's exergy destruction which is calculated as,

$$ED_{total} = ED_{eva} + ED_{cond} + ED_{cas} + ED_{comp,LTC} + ED_{comp,HTC} + ED_{exp,LTC} + ED_{exp,HTC} \tag{5}$$

The exergetic efficiency of the system is calculated as,

$$\eta_{ex} = \frac{W_{total} - ED_{total}}{W_{total}} \tag{6}$$

The equations used for the exergy destruction of an individual component are mentioned in Table 2.

2.3. Economic analysis

The cascade refrigeration system comprises different components and it is important to know the cost of the individual component to determine the total cost of the system. To calculate the total cost of the system, the capital cost of components with maintenance cost, operational cost and the penalty cost pertaining to CO_2 emissions is considered [26]. Eq. (7) is used to calculate the total cost of the plant.

$$\dot{C}_{total} = \sum \dot{C}_c + \dot{C}_o + \dot{C}_{pen} \tag{7}$$

The capital cost ($\dot{C}_c$) of the system components is calculated using the cost functions as mentioned in Table 3. The capital cost and the maintenance cost of the individual component are calculated using Eq. (8),

$$\dot{C}_c = C_c \, x \, \varphi \, x \, CRF \tag{8}$$

where CRF is the capital recovery factor representing the return on the initial invested capital for the lifespan of an investment made. The work of Prajapati et al. [27] is referred to calculate CRF as presented in the Eq. (9),

$$CRF = \frac{i(1+i)^n}{(1+i)^n - 1} \tag{9}$$

The major components of the cascade refrigeration system are considered for the calculation of total capital and maintenance costs as presented in Eq. (10),

$$\sum \dot{C}_c = \dot{C}_{eva} + \dot{C}_{cond} + \dot{C}_{cas} + \dot{C}_{comp,LTC} + \dot{C}_{comp,HTC} + \dot{C}_{exp,LTC} + \dot{C}_{exp,HTC} \tag{10}$$

The operational cost of the system is calculated considering the electricity consumed by the compressor as mentioned in Eq. (11),

Table 3
Cost of the individual system component [28,29].

Component	Capital cost of individual component
Evaporator	$C_{eva} = 1397 \times A_{eva}^{0.89}$
Condenser	$C_{cond} = 1397 \times A_{cond}^{0.89}$
Cascade condenser	$C_{cas} = 383.5 \times A_{cas}^{0.65}$
LTC Compressor	$C_{comp,LTC} = 10167.5 \times W_{LTC}^{0.46}$
HTC Compressor	$C_{comp,HTC} = 9624.2 \times W_{HTC}^{0.46}$
LTC Throttle valve	$C_{exp,LTC} = 114.5 \times \dot{m}_{LTC}$
HTC Throttle valve	$C_{exp,HTC} = 114.5 \times \dot{m}_{HTC}$

$$\dot{C}_o = N\,x\,W_t\,x\,C_{elec} \tag{11}$$

where W_t is the total work consumed by the compressor, N refers to the annual operating hours of the cascade refrigeration system and C_{elec} is the cost of electricity.

2.4. Environmental analysis

The working fluids used in the CRS are responsible for greenhouse gas (GHG) emissions and the penalty cost pertaining to their emission is calculated using Eq. (12) as recommended by Wang et al. [30],

$$\dot{C}_{pen} = m_{CO_{2e}}\,x\,C_{CO_2} \tag{12}$$

The amount of GHG emissions is calculated using Eq. (13),

$$m_{CO_{2e}} = \mu_{CO_{2e}}\,x\,E \tag{13}$$

3. Multi-objective optimization

Most engineering problems are governed by a set of parameters and each parameter affects the system performance in different ways and at times is conflicting in nature [31]. Multi-objective optimization helps in understanding the effect of multiple variables on the objective functions simultaneously and at the same time it provides multiple optimal solutions within the given constraints. Numerous types of metaheuristic-based optimization algorithms are available with diversified exploration and exploitation approaches [32].

Considering the fundamentals of heat transfer and thermodynamics, Patel et al. [33] developed the heat transfer search (HTS) optimization algorithm. In the present work, the HTS optimization algorithm is used to carry out thermo-economic optimization of cascade refrigeration systems using different pairs of refrigerants in LTC and HTC. The employment of multi-objective optimization enables a user to obtain multiple optimal solutions and helps in selecting optimum operating parameters to yield optimum system performance.

The HTS algorithm is based on the laws of thermodynamics and heat transfer wherein a system always aims to attain a thermal equilibrium with the surroundings. The thermal equilibrium can be attained through heat transfer through the modes of conduction, convection and radiation and subsequently an analogy formulated with respect to the engineering problem helps in obtaining optimal solutions. In the following section, the individual phase of the optimization algorithm is explained in brief.

3.1. Conduction phase

Thermal conduction is defined as the heat transfer between two bodies when they are in contact with each other and the energy flow will always take from molecules possessing high-energy to low-energy in the vicinity. The system aims to attain thermal equilibrium with the surroundings using the conduction heat transfer. The conduction phase mimics the fundamental Fourier law of heat conduction. The objective function values are represented by the energy levels of the molecules. After every iteration of the conduction phase, the new solution is updated with the help of Eqs. (14) and (15).

$$S_{y,x}{}' = \begin{cases} S_{z,x} + \left(-P_{cond}^2 A_{k,x}\right), iff\left(S_y\right) > f(S_z) \\ S_{y,x} + \left(-P_{cond}^2 S_{y,x}\right), iff\left(S_y\right) < f(S_z) \end{cases}; if\ g \le g_{max}/CDF \tag{14}$$

$$S_{y,x}{}' = \begin{cases} S_{z,x} + \left(-n_r S_{z,x}\right), iff\left(S_y\right) > f(S_z) \\ S_{y,x} + \left(-n_r S_{y,x}\right), iff\left(S_y\right) < f(S_z) \end{cases}; if\ g > g_{max}/CDF \tag{15}$$

where x represents the arbitrarily selected design variable 1,2,3…m, y = *1,2,3…n,* $y \neq$ z and z is the arbitrarily selected solution from the population. The probability of executing the conduction phase lies in the range of 0 to 0.333 and it is represented by P_{cond}. The number of molecules and their temperature levels is denoted by n and m, respectively. g represents the number of generations. The optimal solution is explored and exploited with the help of the conduction factor which is denoted as *CDF*.

3.2. Convection phase

The heat transfer resulting from the flow of a fluid (liquid or gas) over a body is regarded as heat convection. On the basis of Newton's law of cooling, the system manages to attain thermal equilibrium through heat convection. As per the law, the heat transfer rate is dependent on the temperature difference between the system and the surroundings. For the thermal equilibrium, the best solution is regarded as the surroundings; hence, the system tries to attain the temperature. During the convection phase, the solutions are modified after every iteration using the Eqs. (16) and (17).

$$S_{y,x}{}' = S_{y,x} + P_{conv}(T_{surr} - TCF\,x\,T_{mean}) \tag{16}$$

$$TCF = \begin{cases} abs(P_{conv} - n_r), ifg \le g_{max}/COF \\ round(1 + n_r) + \left(-P_{conv}^2 S_{y,x}\right), ifg > g_{max}/COF \end{cases} \tag{17}$$

where the temperature of the surroundings is represented by T_{surr} and T_{mean} represents the mean system temperature. The probability of executing the convection phase lies within the range of 0.666 to 1 and it is denoted by P_{conv}. Similar to the conduction factor, the convection factor helps in the exploration and exploitation of the optimal solution that is represented by COF and the temperature change factor is represented by TCF.

3.3. Radiation phase

The execution of the radiation phase is based on the interaction of the system (at a higher temperature) and the surroundings (usually at a lower temperature) through the medium of electromagnetic waves. The radiation phase mimics Stephen Boltzman's law as the system makes an attempt to maintain the thermal balance with the surroundings. During the each iteration of the radiation phase, the new solutions are modified using Eqs. (18) and (19)

$$S_{y,x}{}' = \begin{cases} S_{y,x} + P_{rad}\left(S_{z,x} - S_{y,x}\right), iff\left(S_y\right) > f(S_z) \\ S_{y,x} + P_{rad}\left(S_{y,x} - S_{z,x}\right), iff\left(S_y\right) < f(S_z) \end{cases}; if\ g \le g_{max}/RDF \tag{18}$$

$$S_{y,x}{}' = \begin{cases} S_{y,x} + n_r\left(S_{z,x} - S_{y,x}\right), iff\left(S_y\right) > f(S_z) \\ S_{y,x} + n_r\left(S_{y,x} - S_{z,x}\right), iff\left(S_y\right) < f(S_z) \end{cases}; if\ g > g_{max}/RDF \tag{19}$$

The probability of the execution of the radiation phase lies in the range of 0.333 to 0.666 and it is represented by P_{rad}. RDF represents the radiation factor for the exploration and exploitation of the optimal solution from the workspace.

3.4. Objective function formulation

The focus of the study is to perform a thermo-economic optimization of a cascade refrigeration system. Two different pair of refrigerants are considered for the study and it is of interest to maximize the COP of the system and at the same time minimize the total cost of the system. The coefficient of performance (COP) and the total cost of the cascade refrigeration system are calculated using Eqs. (3) and (7), respectively. Table 4 summarizes the input design parameters for the investigation. The effects of the evaporation temperature (T_{eva}), the condensation temperature (T_{cond}), LTC condenser temperature (T_{LTC}) and cascade condenser temperature difference (dT) on the objective functions are studied and presented. The decision variables and their range during optimization is tabulated in Table 5.

In the mathematical form, the multi-objective optimization problem is formulated as,

Table 4
Input parameters for the multi-objective optimization.

Input Parameter	Value, Unit
Ambient temperature	25 ℃
Cooling load	50 kW
Compressor isentropic efficiency	80 %
Compressor mechanical efficiency	100 %
Compressor electrical efficiency	100 %
Superheating in LTC	5 K
Superheating in HTC	5 K
Overall heat transfer coefficient in evaporator	0.03 kW/m^{2}K
Overall heat transfer coefficient in condenser	0.04 kW/m^{2}K
Overall heat transfer coefficient in cascade condenser	1 kW/m^{2}K
Inlet temperature of air to the evaporator	263 K
Maintenance factor	1.06
Interest rate	14 %
Plant life	15 years
Operational hour	4266 h
Electrical unit cost	0.09 USD/kWh
Emission factor	0.968 kg/kWh
Cost of CO_2	0.09 USD/kg of CO_2 emission

Table 5
Bounds of design variables for optimization.

Design Variable	Lower Bound	Upper Bound
Evaporation temperature, *K*	223	252
Condensation temperature, *K*	236	218
LTC condenser temperature, *K*	267	279
Cascade condenser temperature difference, *K*	2	8

$$Z_1 = \textbf{maximize}\,\mathrm{COP}\ (X),\ \text{where}\ X = [x_1,\ x_2,\ x_3, x_4], x_{i,\min} \le x_i \le x_{i,\max}; i = 1, 2, 3, 4 \tag{20}$$

$$Z_2 = \textbf{minimize}\,\dot{C}_{\text{total}}(Y),\ \text{where}\ Y = [y_1,\ y_2,\ y_3,\ y_4], y_{i,\min} \le y_i \le y_{i,\max}; i = 1, 2, 3, 4 \tag{21}$$

Where Z_1 and Z_2 are the identified objective functions to optimize for the CRS.

3.5. Multi-criteria decision making

In the present investigation, multiple optimal solutions are obtained with the help of the HTS optimization algorithm and the Pareto curve representing the solutions is obtained. It is also observed that the objective functions are conflicting in nature and any attempt to increase the impact of one objective function, the other objective function gets affected in a negative manner. For example, in an attempt to increase the exergy efficiency of the CRS, the total cost of the system increases and vice versa. In such a situation, multi-criteria decision-making (MCDM) techniques enable a user to select the best suitable point among multiple solutions [34,35,36]. The Technique for Order Preference by Similarity to Ideal Solution (TOPSIS) is one such conventional MCDM technique to identify the best solution among numerous optimal solutions available [37]. The technique helps in making analytical decisions based on the available dataset [38,39].

The process of making a decision using TOPSIS involves analysis of pre-collected numerical data, assigning respective weights and employing reliable metrics to the data [40]. An evaluation matrix comprising $\boldsymbol{x}$ number of possible alternatives and $\boldsymbol{y}$ number of criteria is developed. The normalization process of the evaluation matrix is performed and weights are assigned. The weighted matrix is formed by multiplying the mass factor with the normalized matrix. Subsequently, the positive and negative solutions are identified with respect to the ideal solution and the relative closeness of each solution is identified. The relative closeness of each solution is ranked and the highest values give the ideal solution for the given scenario [41]. The detailed process flowchart of the TOPSIS methodology is presented using the flowchart in Fig. 3.

4. Results and discussion

The multi-objective optimization results for the CRS is presented and discussed in this section. The Pareto front comprising of optimal solutions is presented for both the pairs of refrigerant i.e. R41-R600a and R170-R600a. TOPSIS criteria is employed to select the best suitable solution and correspondingly design parameters are identified to yield optimum system performance. The effect of design variables on the COP and the total cost of the system is investigated and presented in the current section.

4.1. Pareto front

The HTS optimization algorithm is employed to optimize the objective functions within the given range of design variables and multiple optimal points are presented using the Pareto optimal curve. The Pareto optimal curve for refrigerant pairs R41-R600a and R170-R600a is presented in Fig. 4. It is observed from the results that, with any effort made to increase the exergy efficiency of the CRS, the total cost of the system increases. Similarly, with any effort made to reduce the cost of the CRS, the exergy efficiency decreases.

On the Pareto optimal curve, five points *(A)* to *(E)* are identified and their effect on the objective functions is discussed. The sensitivity analysis with respect to the individual optimal point is carried out and the variation in COP and the total cost is studied. The optimal point *(A)* and *(E)* corresponds to the condition of minimum total cost and maximum COP of the CRS, respectively. The Pareto optimal curve for refrigerant pair R41-R600a shows improved performance as compared to R170-R600a. At any optimal point on the Pareto front, for the same total cost of the system, exergy efficiency is always higher for the system operated with the refrigerant pair R41-R600a than R170-R600a.

The values of design variables pertaining to key optimal points from the Pareto curve *(A)* – *(E)* and the TOPSIS point are tabulated in Table 6. For the refrigerant pair R41-R600a and R170-R600a the maximum exergy efficiency of the system is 64.4 % and 63.3 %. Whereas, the total cost of the system when the system operates at maximum exergy efficiency is 80,110 $/year and 79,912 $/year, respectively. It is also observed from the results that the effect of evaporation and condensation temperature and LTC condenser temperature is profound on the exergy efficiency and total cost of the system. However, the effect of cascade temperature difference is not significant in obtaining optimum results. Among the multiple optimal solutions, the most suitable operating condition is identified using the TOPSIS selection criteria and the optimum exergy efficiency and the total cost of the CRS is 63.5 % and 65,228 $/year for the refrigerant pair R41-R600a.

4.2. Result validation

The multi-objective optimization results of the current study are compared with the results of the existing literature [20] to validate the thermodynamic and economic model. The optimization problem is considered as a benchmark to compare the results where the objective is to maximize the exergy efficiency and minimize the total cost of CRS. The constraints and the input boundary conditions are similar to the reference study with the only change in the working fluid. The refrigerant pair R170-R404a and R41-R404a is used in the reference study [20] whereas, the refrigerant pair R170-R600a and R41-R600a is used in the current investigation. The refrigerant R404a is replaced by safe and less hazardous environment-friendly refrigerant R600a to reduce the environmental impact and CO_2 penalty.

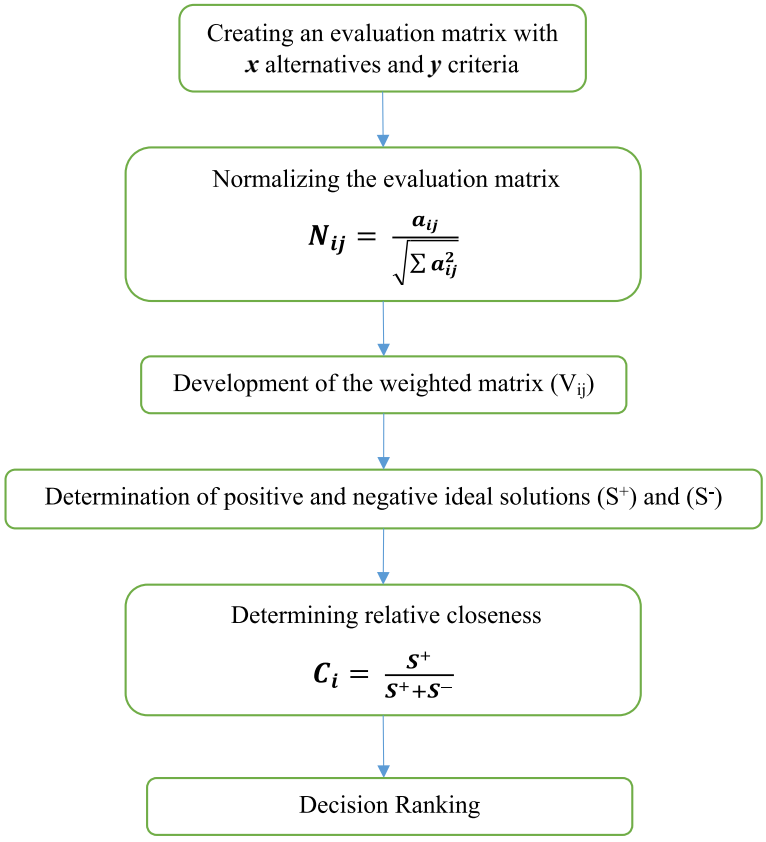

Fig. 3. Flow chart of TOPSIS methodology.

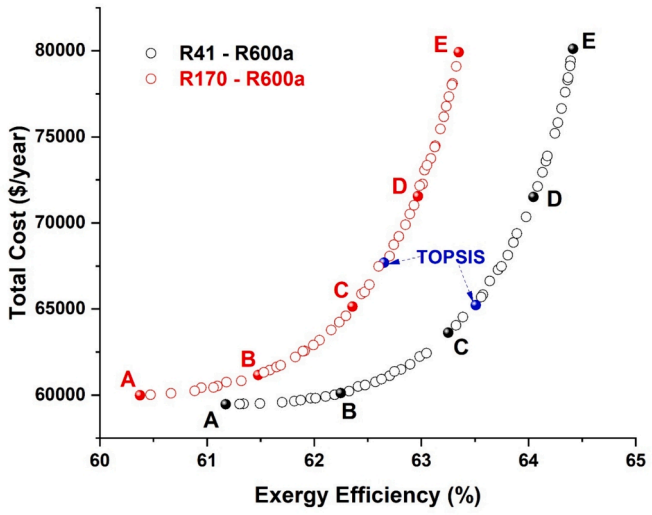

Fig. 4. Pareto optimal curve from multi-objective optimization of the CRS.

The comparative result is presented using the Pareto optimal curve for all the refrigerant pairs and is presented in Fig. 5. The optimization results obtained are in good agreement with the results from the reference study and hold a solid motivation to carry out a detailed thermo-economic analysis of the CRS. The GWP of refrigerant R404a is 3800 whereas for the refrigerant R600a, GWP is 3. The less hazardous refrigerant R600a is a suitable replacement of R404a in the HTC of the CRS showing better thermal and economic performance. The CRS system operating with the refrigerant pair R41-R600 yields the highest exergy efficiency at any given total cost and vice versa. The optimum value of the decision variables for the refrigerant pairs used from the reference and the current study is tabulated in Table 7. The highest exergy efficiency of the CRS is obtained as 63.5 % with the refrigerant pair R41-R600a.

4.3. *Effect of design variables*

In the current section, the effect of individual design variables on the total cost and the exergy efficiency of the CRS is investigated and presented for both the pair of refrigerants. Fig. 6 represents the variation in exergy efficiency and total cost of CRS with respect to the evaporation temperature which is varied from 223 K to 252 K. It is observed that, with the increase in the evaporation temperature, the exergy efficiency increases. The maximum exergy efficiency of 63.8 % and 62.8 % is obtained at evaporation temperature 252 K for the refrigerant pair R41-R600a and R170-R600a, respectively.

With the increase in the evaporation temperature, the total plant cost decreases because the compressor load reduces and hence the compressor input power. Correspondingly, lower input power leads to a reduction in operating costs and CO2 penalty costs. Beyond a certain evaporation temperature (−31 °C or 242 K), the capital costs increase owing to the increased heat transfer surface area of the evaporator. An increase in heat exchanger size resembles an increase in capital cost and operational cost. The minimum total cost of the system is obtained as 62,764 $/year and 64,043 $/year at the evaporation temperature −31.3°C for the refrigerant pair R41-R600a and R170-R600a, respectively. At the condition when the system operates at minimum cost, the exergy efficiency of the CRS is 62.6 % and 61.7 % for the refrigerant pair R41-R600a and R170-R600a, respectively. Hence, any attempt made to reduce the cost of the system, the exergy efficiency of the system is

Table 6
Value of design variables for optimal points *(A)* – *(E)* during multi-objective optimization.

Variables/Objective Functions	R41-R600a						R170-R600a					
	A	B	C	D	E	TOPSIS	A	B	C	D	E	TOPSIS
Evaporation temperature, K	241	243.6	246.4	251.2	252	**248.4**	241.4	243.7	246.6	250.3	252	**249.6**
Condenser temperature, *K*	321.7	319.4	314.5	312.5	310	**314.3**	321.8	317	313.3	311.6	310	**313.4**
LTC condenser temperature, *K*	267.3	272.4	273.5	273.8	273.5	**273.5**	267	267.7	268.4	269.3	269.7	**269.5**
Cascade condenser temperature difference, *K*	2	2	2	2	2	**2**	2	2	2	2	2	**2**
Exergy efficiency, %	**61.2**	62.2	63.3	64	**64.4**	**63.5**	**60.4**	61.5	62.4	63	**63.3**	**62.6**
Total cost of the system, $/year	**59,462**	60,111	63,621	71,511	**80,110**	**65,228**	**59,984**	61,160	65,142	71,543	**79,912**	**67,690**

The values in the bold represent the maximum and minimum value of both the objective functions at point A & E. Similarly, the ideal operating condition as selected by TOPSIS criterion is highlighted in bold.

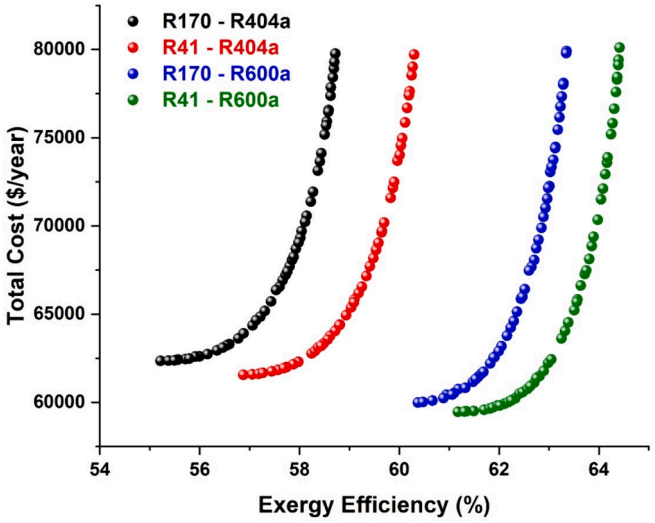

Fig. 5. Validation of the multi-objective optimization results.

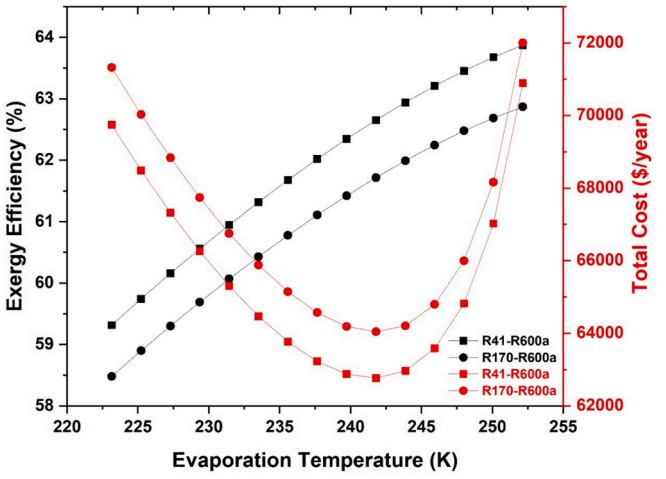

Fig. 6. Effect of the evaporation temperature on the exergy efficiency and total cost of CRS.

Table 7
Optimum value of the objective functions obtained by TOPSIS criteria for the existing and the current study.

	R170–404a	R41–R404a	R170–R600a	R41-R600a
Evaporator Temperature, K	235.1	235.4	249.6	248.4
Condenser Temperature, K	319.5	320.2	313.4	314.3
LTC condenser Temperature, K	273	280.8	269.5	273.5
Cascade condenser temperature difference, K	2.1	2.1	2	2
Exergy Efficiency, %	54.9	56.2	62.6	63.5
Total Cost, $/year	64,808	63,346	67,690	65,228

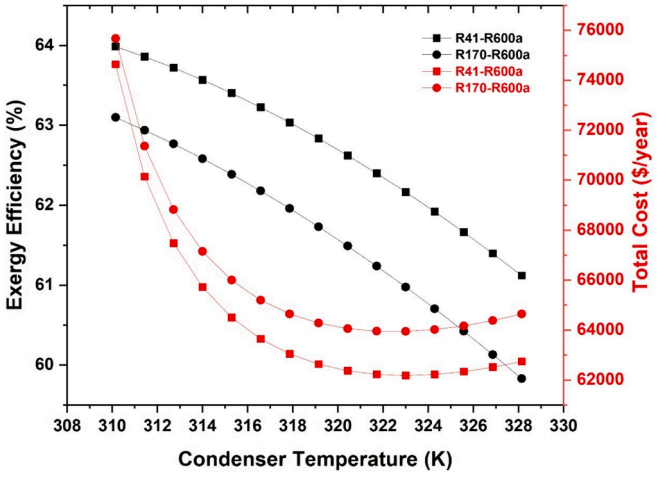

Fig. 7. Effect of the condenser temperature on the exergy efficiency and total cost of CRS.

compromised and vice-versa.

The effect of the condenser temperature on the total cost and exergy efficiency of the CRS is presented in Fig. 7. The effect of the condenser temperature is considered for the range 310 K to 328 K. The increase in the condenser temperature from, 310 K to 328 K results in the reduction of exergy efficiency from 63.9 % to 61.1 % for the refrigerant pair R41-R600a and 63 % to 59.8 % for R170-R600a. The increase in the condenser temperature results in the increase in pressure ratio in the HTC and eventually increases the total power consumed by the compressor.

With the increase in the condenser temperature, the total cost of the system decreases gradually, reaches to the minimum total cost and after a certain condenser temperature (223.2 K), the total cost of CRS starts to increase. The reduction in cost corresponds to reduced condenser size due to increased heat transfer coefficient in the condenser, eventually reducing the capital, maintenance and operating costs. The minimum cost of the CRS is obtained as 62,182 $/year and 63,945 $/year at condenser temperature 223.2 K for the refrigerant pair R41-R600a and R170-R600a, respectively.

The variation in exergy efficiency and total cost of the system with respect to the change in LTC condenser temperature is presented in Fig. 8. The LTC condenser temperature is varied from 267 K to 279 K and

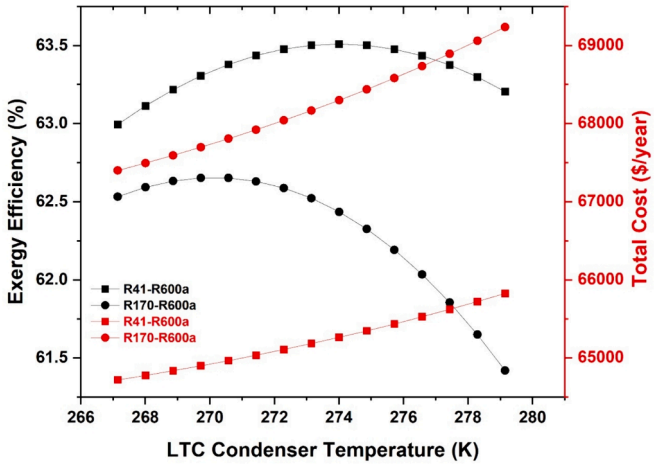

Fig. 8. Effect of the LTC condenser temperature on the exergy efficiency and total cost of CRS.

it is observed that an increase in the condenser temperature increases the exergy efficiency, however, beyond a certain condenser temperature, the efficiency decreases and drops to the minimum exergy efficiency at 279 K. The maximum exergy efficiency of 63.5 % and 62.6 % is obtained for the refrigerant paint R41-R600a and R170-R600a, at the LTC condenser temperature 273.8 K and 270.4 K, respectively. The increase in the LTC condenser temperature results in an increased pressure ratio in the LTC and a decrease in the HTC. As a result, the input compressor work increases in the LTC and reduces in the HTC. The decrease in the compressor work accounts for the increase in the exergy efficiency of the system up to the optimum condition.

The increase in LTC condenser temperature results in increasing the total cost of the system which is evident from the results. There is a substantial difference in the total cost of the system for the refrigerant pair R41-R600a as compared to R170-R600a. The minimum total cost of the system is 64,719 $/year and 67,399 $/year for the refrigerant pair R41-R600a and R170-R600a respectively at LTC condenser temperature 267 K.

Fig. 9 represents the variation in the exergy efficiency and total cost of the CRS with respect to the cascade condenser temperature difference. The range of cascade condenser temperature difference is varied from 2 K to 8 K and its effect on the objective function is studied. The results depict the linear relationship between the variables and with increase in the temperature difference will result in increase in the total cost of the system and decrease in the exergy efficiency. The optimum performance of the system is obtained at condenser temperature difference of 2 K when the exergy efficiency is maximum at 63.5 % and 62.6 % and the total cost is minimum at 65,228 $/year and 67,690 $/year for the refrigerant pair R41-R600a and R170-R600a, respectively.

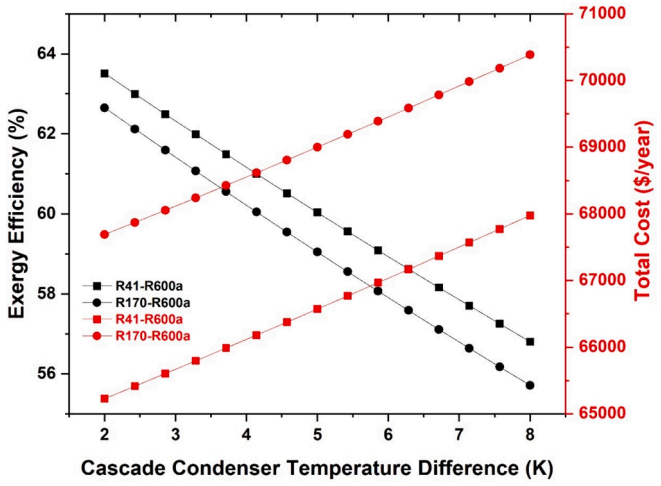

Fig. 9. Effect of the cascade condenser temperature difference on the exergy efficiency and total cost of CRS.

4.4. Economic analysis

The economic analysis is carried out to understand the distribution of total cost of the system among various components. The total cost of the plant includes, the capital cost, operation and maintenance cost and penalty cost with reference to the CO_2 emissions. The distribution of the cost of the components responsible for the total cost of the system at TOPSIS point is presented in Fig. 10 for the refrigerant pair R170-R600a and R41-R600a. The total cost of the system using the refrigerant pair R170-R600a and R41-R600a at TOPSIS point is 67,690 $/year and 65,228 $/year, respectively. The major fraction of the cost is due to the capital cost of condenser and evaporator in both the cases which is 29.9 % and 31.7 % for the refrigerant pair R170-R00a and 29.4 % and 29.9 % for R41-R600a, respectively. The CO_2 penalty cost corresponds to 11.6 % and 12.3 % of the total cost with the respective refrigerant pairs. The cost of cascade condenser and the expansion valves in HTC and LTC is almost negligible with respect to the total cost of CRS.

The cost of the compressor in HTC and LTC corresponds to 8.5 % and 6 % of the total cost of the system. Continuous operation and maintenance of the system is ensured and the corresponding cost is calculated for the system. For the refrigerant pair R170-R600a, the operating cost is 11.6 % of the total cost whereas it is 12.7 % for the CRS operating with R41-R600a. The distribution of the cost for the components of CRS at each optimal points on the Pareto optimal curve *(A) – (E)* is presented in the Fig. 11 for the refrigerant pairs R170-R600a and R41-R600a.

4.5. Population distribution of design variables

Fig. 12(a)–(d) represents the distribution of the design variables during the multi-objective optimization. The maximum and minimum limit of an individual design variable is tabulated in Table 5. From the scattered distribution of variables, it is observed that the effect of the evaporation temperature, condensation temperature and the LTC condenser temperature is profound in obtaining the optimal solution. The population distribution is evenly scattered across the design variable range. The exergy efficiency and the total cost of the system are sensitive to these design variables. However, the effect of the cascade condenser temperature difference on the system performance is not significant as it converges to a single value. Any change in the

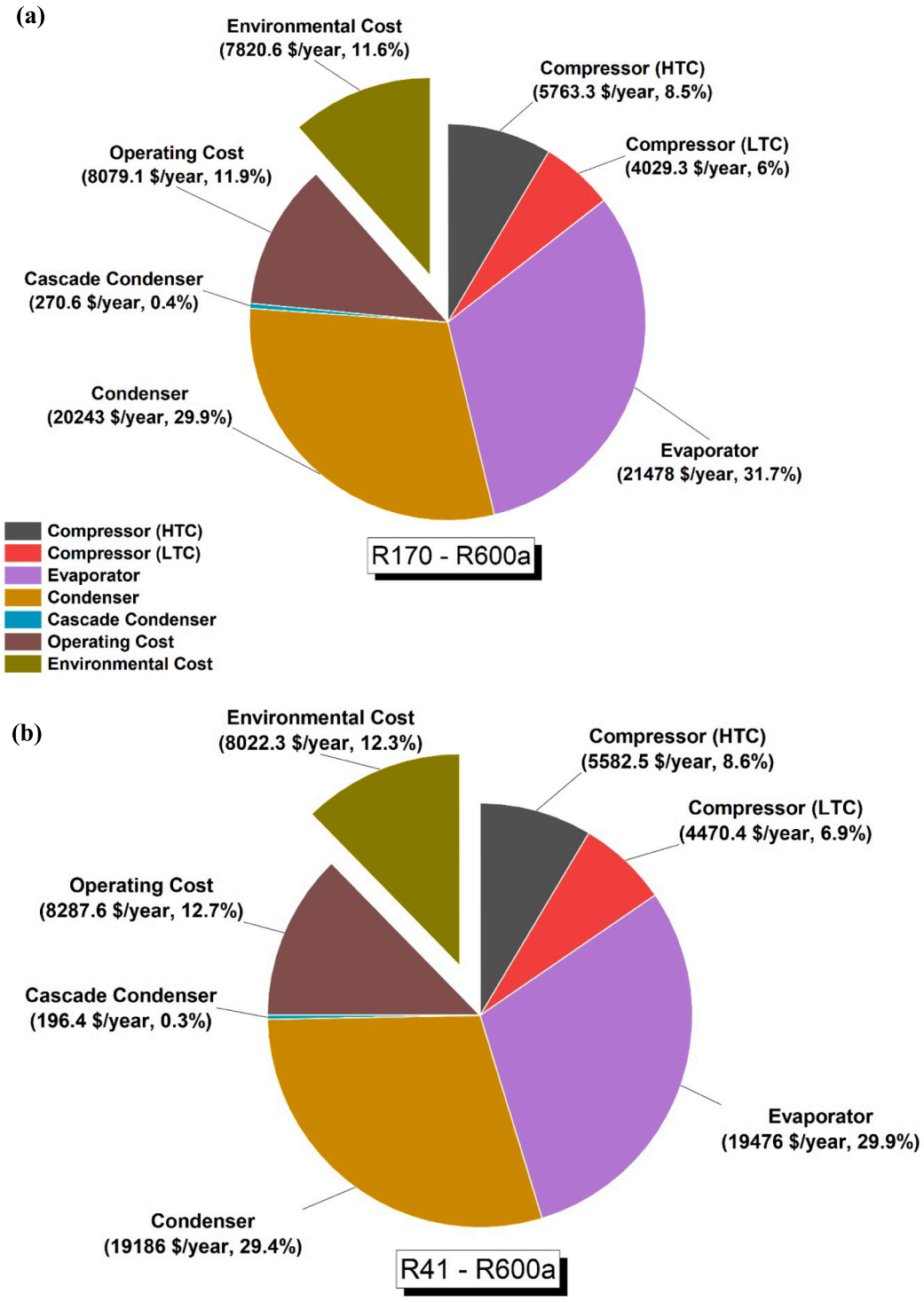

Fig. 10. Distribution of cost of the system components at TOPSIS point (a) R170 – R600a and (b) R41-R600a.

temperature difference will result in reducing the system's performance.

5. Conclusions

The current study deals with energy-exergy-economic-environmental (4E) analysis and multi-objective optimization of a cascade refrigeration system with the objective to maximize the exergy efficiency and minimize the total cost of the system. Two sets of refrigerant pairs are used for the study R41-R600a and R170-R600a considering the environment-friendly nature. R600a is used as a working fluid in HTC because of its very low GWP. Heat transfer search optimization algorithm is used to optimize the objective functions and obtain a set of multiple optimal solutions. TOPSIS decision-making technique is used to select the ideal solution.

At any optimal point on the Pareto front, for the same total cost of the system, exergy efficiency is always higher for the system operated with the refrigerant pair R41-R600a than R170-R600a. Among the several multiple optimal solutions, the most suitable operating condition is

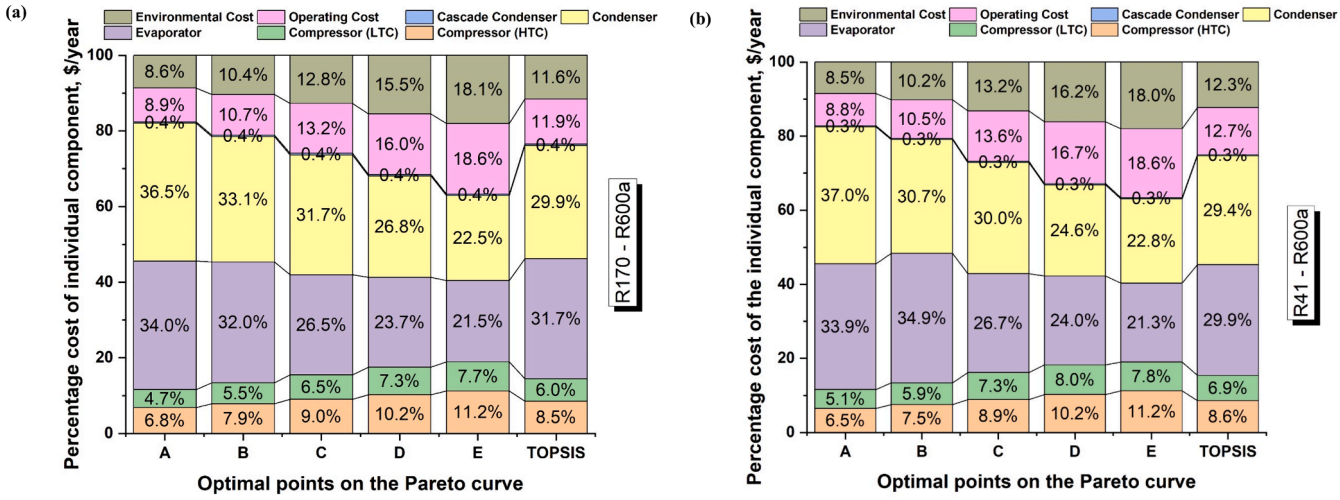

Fig. 11. Percentage cost distribution of the CRS components at the optimal points (A) – (E) and TOPSIS point for (a) R170-R600a and (b) R41-R600a.

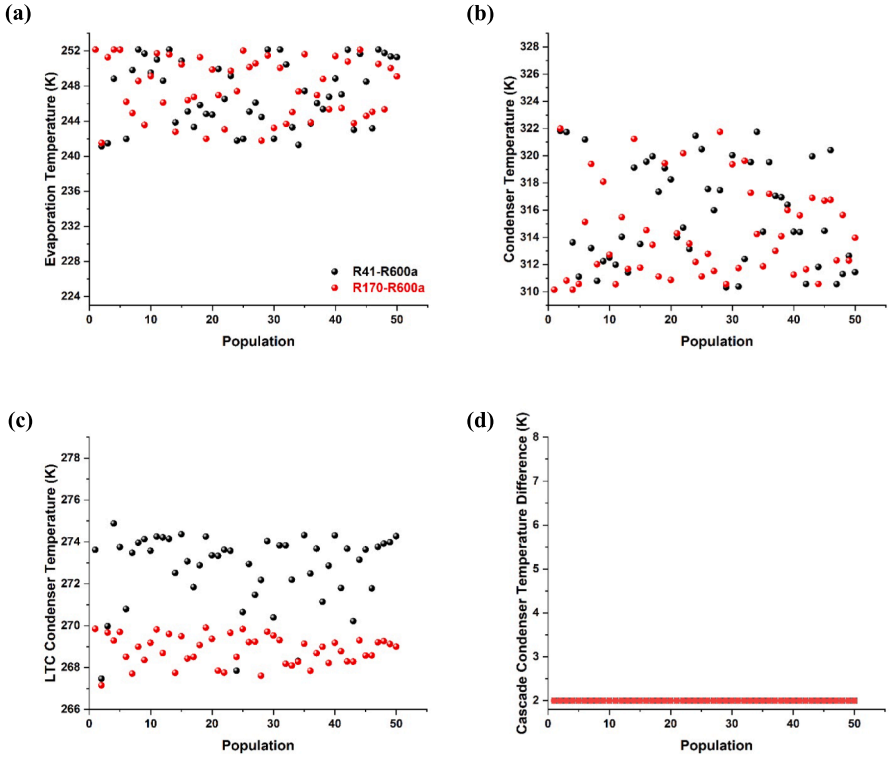

Fig. 12. Distribution of the design variables (a) evaporation temperature, (b) condenser temperature, (c) LTC condenser temperature, and (d) cascade condenser temperature difference.

identified using the TOPSIS selection criteria and the optimum exergy efficiency and the total cost of the CRS is 63.5 % and 65,228 $/year for the refrigerant pair R41-R600a. With the increase in evaporator temperature, the exergy efficiency of the CRS increases whereas, it decreases with the increase in the condenser temperature. The major fraction of the total cost of CRS is due to the capital cost of the condenser and evaporator which is 29.4 % and 29.9 % for R41-R600a; whereas, the CO_2 penalty cost corresponds to 12.3 %. It is also observed that the effect of evaporation and condensation temperature and LTC condenser temperature is profound on the exergy efficiency and total cost of the system. The effect of cascade condenser temperature difference is observed to be linear and optimum results obtained at the difference of 2 °C. The scattered distribution of variables shows the profound effect of the evaporation temperature, condensation temperature and the LTC condenser temperature to obtain optimal solutions.

CRediT authorship contribution statement

Parth Prajapati: . **Vivek Patel:** Validation, Methodology, Investigation, Conceptualization. **Bansi D. Raja:** Writing – review & editing, Validation. **Hussam Jouhara:** Writing – review & editing.

Declaration of competing interest

The authors declare that they have no known competing financial interests or personal relationships that could have appeared to influence the work reported in this paper.

Data availability

No data was used for the research described in the article.

Acknowledgement

The work is done as part of the collaboration between Pandit Deendayal Energy University and the Heat Pipe and Thermal Management Research Group at Brunel University London, UK.

References

[1] M. Hosoz, H.M. Ertunc, Modelling of a cascade refrigeration system using artificial neural network, Int. J. Energy Res. 30 (14) (2006) 1200–1215, https://doi.org/10.1002/er.1218.
[2] M. Pan, H. Zhao, D. Liang, Y. Zhu, Y. Liang, G. Bao, A review of the cascade refrigeration system, Energies 13 (2020) 2254, doi: 10.3390/EN13092254.
[3] H. Jouhara, T. Nannou, H. Ghazal, R. Kayyali, S.A. Tassou, S. Lester, Temperature and energy performance of open refrigerated display cabinets using heat pipe shelves, Energy Procedia 123 (2017) 273–280, https://doi.org/10.1016/J.EGYPRO.2017.07.240.
[4] H. Jouhara, et al., Low-temperature heat transfer mediums for cryogenic applications, J. Taiwan Inst. Chem. Eng. (2023) 104709, https://doi.org/10.1016/J.JTICE.2023.104709.
[5] M.W. Faruque, M.R. Uddin, S. Salehin, M.M. Ehsan, A comprehensive thermodynamic assessment of cascade refrigeration system utilizing low GWP hydrocarbon refrigerants, Int. J. Thermofluids 15 (2022) 100177, https://doi.org/10.1016/J.IJFT.2022.100177.
[6] T. Aized et al., Energy and Exergy Analysis of Vapor Compression Refrigeration System with Low-GWP refrigerants, Energies 15 (2022) 7246, doi: 10.3390/EN15197246.
[7] J. Wajs, M. Mrozek, E. Fornalik-Wajs, Combined cold supply system for ship application based on low GWP refrigerants – Thermo-economic and ecological analyses, Energ. Conver. Manage. 258 (2022) 115518, https://doi.org/10.1016/J.ENCONMAN.2022.115518.
[8] A. Kumar, M. R. Chen, K. S. Hung, C. C. Liu, and C. C. Wang, "A Comprehensive Review Regarding Condensation of Low-GWP Refrigerants for Some Major Alternatives of R-134a," Processes 10 (9) (2022) 1882, Sep. 2022, doi: 10.3390/PR10091882.
[9] P. Singha, M.S. Dasgupta, S. Bhattacharyya, A. Hafner, Energy, environmental, and economic analysis of novel R744/R290 cascade refrigeration systems designed for warm ambient conditions utilizing ejector, Therm. Sci. Eng. Prog. 53 (2024) 102724, https://doi.org/10.1016/j.tsep.2024.102724.
[10] L.H.P. Massuchetto, R.B.C. do Nascimento, S.M.R. de Carvalho, H.V. de Araújo, J. V.H. d'Angelo, Thermodynamic performance evaluation of a cascade refrigeration system with mixed refrigerants: R744/R1270, R744/R717 and R744/RE170, Int. J. Refrig 106 (2019) 201–212, https://doi.org/10.1016/J.IJREFRIG.2019.07.005.
[11] A. Ustaoglu, B. Kursuncu, M. Alptekin, M.S. Gok, Performance optimization and parametric evaluation of the cascade vapor compression refrigeration cycle using Taguchi and ANOVA methods, Appl. Therm. Eng. 180 (2020) 115816, https://doi.org/10.1016/J.APPLTHERMALENG.2020.115816.
[12] Y. Zhang, Y. He, Y. Wang, X. Wu, M. Jia, Y. Gong, Experimental investigation of the performance of an R1270/CO2 cascade refrigerant system, Int. J. Refrig 114 (2020) 175–180, https://doi.org/10.1016/J.IJREFRIG.2020.02.017.
[13] K. Golbaten Mofrad, S. Zandi, G. Salehi, M.H. Khoshgoftar Manesh, 4E analyses and multi-objective optimization of cascade refrigeration cycles with heat recovery system, Therm. Sci. Eng. Prog. 19 (2020) 100613, https://doi.org/10.1016/j.tsep.2020.100613.
[14] M. Deymi-Dashtebayaz, A. Sulin, T. Ryabova, I. Sankina, M. Farahnak, R. Nazeri, Energy, exergoeconomic and environmental optimization of a cascade refrigeration system using different low GWP refrigerants, J. Environ. Chem. Eng. 9 (6) (Dec. 2021) 106473, https://doi.org/10.1016/J.JECE.2021.106473.
[15] F. Yilmaz, R. Selbaş, Energy and exergy analyses of CO2/HFE7000 cascade cooling system, Süleyman Demirel Univ. J. Nat. Appl. Sci. 21 (3) (Oct. 2017) 854–860, https://doi.org/10.19113/SDUFBED.58140.
[16] F. Yilmaz, R. Selbaş, Comparative thermodynamic performance analysis of a cascade system for cooling and heating applications, Int. J. Green Energy 16 (9) (Jul. 2019) 674–686, https://doi.org/10.1080/15435075.2019.1618308.
[17] M. Walid Faruque, M. Hafiz Nabil, M. Raihan Uddin, M. Monjurul Ehsan, S. Salehin, Thermodynamic assessment of a triple cascade refrigeration system utilizing hydrocarbon refrigerants for ultra-low temperature applications, Energ. Conver. Manage. X 14 (2022) 100207, https://doi.org/10.1016/J.ECMX.2022.100207.
[18] K. Kumar Singh, R. Kumar, A. Gupta, Comparative energy, exergy and economic analysis of a cascade refrigeration system incorporated with flash tank (HTC) and a flash intercooler with indirect subcooler (LTC) using natural refrigerant couples, Sustainable Energy Technol. Assess. 39 (Jun. 2020) 100716, https://doi.org/10.1016/J.SETA.2020.100716.
[19] J. Gill, J. Singh, O.S. Ohunakin, D.S. Adelekan, Exergy analysis of vapor compression refrigeration system using R450A as a replacement of R134a, J. Therm. Anal. Calorim. 136 (2) (Apr. 2019) 857–872, https://doi.org/10.1007/S10973-018-7675-Z/FIGURES/12.
[20] R. Roy, B.K. Mandal, Thermo-economic analysis and multi-objective optimization of vapour cascade refrigeration system using different refrigerant combinations: A comparative study, J. Therm. Anal. Calorim. 139 (5) (2020) 3247–3261, https://doi.org/10.1007/s10973-019-08710-x.
[21] Z. Sun, Y. Wang, Comprehensive performance analysis of cascade refrigeration system with two-stage compression for industrial refrigeration, Case Stud. Therm. Eng. 39 (Nov. 2022) 102400, https://doi.org/10.1016/J.CSITE.2022.102400.
[22] J. Gill, J. Singh, O.S. Ohunakin, D.S. Adelekan, ANN approach for irreversibility analysis of vapor compression refrigeration system using R134a/LPG blend as replacement of R134a, J. Therm. Anal. Calorim. 135 (4) (Feb. 2019) 2495–2511, https://doi.org/10.1007/S10973-018-7437-Y/FIGURES/19.
[23] M.A.B. Yunus, A. Cengel, Thermodynamics: an engineering approach, 8th ed., McGraw-Hill, 2015.
[24] J.J. Fierro, et al., Exergo-economic comparison of waste heat recovery cycles for a cement industry case study, Energy Convers. Manage.: X 13 (Jan. 2022) 100180, https://doi.org/10.1016/J.ECMX.2022.100180.
[25] C. Aktemur, I.T. Ozturk, C. Cimsit, Comparative energy and exergy analysis of a subcritical cascade refrigeration system using low global warming potential refrigerants, Appl. Therm. Eng. 184 (2021) 116254, https://doi.org/10.1016/J.APPLTHERMALENG.2020.116254.
[26] M. Mehrpooya, B. Ghorbani, S.A. Mousavi, A. Zaitsev, Proposal and assessment of a new integrated liquefied natural gas generation process with auto – Cascade refrigeration (exergy and economic analyses), Sustainable Energy Technol. Assess. 40 (2020) 100728, https://doi.org/10.1016/J.SETA.2020.100728.
[27] P.P. Prajapati, V.K. Patel, Thermo-economic optimization of a nanofluid based organic Rankine cycle: A multi-objective study and analysis, Therm. Sci. Eng. Prog. 17 (2020), https://doi.org/10.1016/j.tsep.2019.100381.
[28] M. Aminyavari, B. Najafi, A. Shirazi, F. Rinaldi, Exergetic, economic and environmental (3E) analyses, and multi-objective optimization of a CO2/NH3 cascade refrigeration system, Appl. Therm. Eng. 65 (1–2) (2014) 42–50, https://doi.org/10.1016/j.applthermaleng.2013.12.075.
[29] O. Rezayan, A. Behbahaninia, Thermoeconomic optimization and exergy analysis of CO2/NH3 cascade refrigeration systems, Energy 36 (2) (2011) 888–895, https://doi.org/10.1016/j.energy.2010.12.022.
[30] J. Wang, Z.J. Zhai, Y. Jing, C. Zhang, Particle swarm optimization for redundant building cooling heating and power system, Appl. Energy 87 (12) (2010) 3668–3679, https://doi.org/10.1016/J.APENERGY.2010.06.021.
[31] V. K. Patel, B. D. Raja, P. Prajapati, L. Parmar, and H. Jouhara, "An investigation to identify the performance of cascade refrigeration system by adopting high-temperature circuit refrigerant R1233zd (E) over R161," *International Journal of Thermofluids*, vol. 17, no. December 2022, p. 100297, 2023, doi: 10.1016/j.ijft.2023.100297.
[32] P.P. Prajapati, V.K. Patel, Comparative analysis of nanofluid-based Organic Rankine Cycle through thermoeconomic optimization, Heat Transfer Asian Res. 48 (7) (2019) 3013–3038, https://doi.org/10.1002/htj.21528.
[33] V.K. Patel, V.J. Savsani, Heat transfer search (HTS): a novel optimization algorithm, Inf. Sci. 324 (2015) 217–246, https://doi.org/10.1016/J.INS.2015.06.044.
[34] Y.A.A. Laouid, C. Kezrane, Y. Lasbet, A. Pesyridis, Towards improvement of waste heat recovery systems: A multi-objective optimization of different organic Rankine cycle configurations, Int. J. Thermofluids 11 (2021) 100100, https://doi.org/10.1016/J.IJFT.2021.100100.
[35] H. Aljaghoub, F. Abumadi, M.N. AlMallahi, K. Obaideen, A.H. Alami, Solar PV cleaning techniques contribute to Sustainable Development Goals (SDGs) using multi-criteria decision-making (MCDM): assessment and review, Int. J. Thermofluids 16 (2022) 100233, https://doi.org/10.1016/J.IJFT.2022.100233.
[36] P. Prajapati, V. Patel, H. Jouhara, An efficient optimization of an irreversible Ericsson refrigeration cycle based on thermo-ecological criteria, Therm. Sci. Eng. Prog. (2022) 101381, https://doi.org/10.1016/J.TSEP.2022.101381.
[37] C.-L. Hwang, K. Yoon, Multiple Attribute Decision Making, 1st ed., vol. 186. In: Lecture Notes in Economics and Mathematical Systems, vol. 186. Berlin, Heidelberg: Springer Berlin Heidelberg, 1981. doi: 10.1007/978-3-642-48318-9.
[38] M.A. Alao, T.R. Ayodele, A.S.O. Ogunjuyigbe, O.M. Popoola, Multi-criteria decision based waste to energy technology selection using entropy-weighted TOPSIS technique: the case study of Lagos, Nigeria, Energy 201 (2020) 117675, https://doi.org/10.1016/J.ENERGY.2020.117675.
[39] N. Mao, M. Song, D. Pan, S. Deng, Comparative studies on using RSM and TOPSIS methods to optimize residential air conditioning systems, Energy 144 (2018) 98–109, https://doi.org/10.1016/J.ENERGY.2017.11.160.
[40] P. Prajapati, V. Patel, B.D. Raja, H. Jouhara, Thermal efficiency and specific work optimization of combined Brayton and inverse Brayton cycle: A multi-objective approach, Therm. Sci. Eng. Prog. 37 (December) (2023) 101624, https://doi.org/10.1016/j.tsep.2022.101624.
[41] K.F.A.D. Dhananj, M.J.V.D.Y. Pimenov, K.G.P.P.R.C., S. Wojciechowski, Integration of Fuzzy AHP and fuzzy TOPSIS methods for wire using RSM, Materials 14 (2021) 7408.